Available online at www.sciencedirect.com
SCIENCE DIRECT®
Advances in Space Research 37 (2006) 1944–1949
ADVANCES IN SPACE RESEARCH (a COSPAR publication)
www.elsevier.com/locate/asr

The energy spectra of heavy nuclei measured by the ATIC experiment

A.D. Panov [a,*], J.H. Adams Jr. [b], H.S. Ahn [c], G.L. Bashindzhagyan [a], K.E. Batkov [a], J. Chang [d,g], M. Christl [b], A.R. Fazely [e], O. Ganel [c], R.M. Gunasingha [e], T.G. Guzik [f], J. Isbert [f], K.C. Kim [c], E.N. Kouznetsov [a], M.I. Panasyuk [a], W.K.H. Schmidt [d], E.S. Seo [c], N.V. Sokolskaya [a], J.P. Wefel [f], J. Wu [c], V.I. Zatsepin [a]

[a] *Skobeltsyn Institute of Nuclear Physics, Moscow State University, Leninskie Gory, Moscow 119992, Russia*
[b] *NASA Marshall Space Flight Center, Huntsville, AL 35812, USA*
[c] *Institute for Physical Science and Technology, University of Maryland, College Park, MD 20742, USA*
[d] *Max Plank Institute fur Aeronomie, Katlinberg – Lindau 37191, Germany*
[e] *Department of Physics, Southern University, Baton Rouge, LA 70813, USA*
[f] *Department of Physics and Astronomy, Louisiana State University, Baton Rouge, LA 70803, USA*
[g] *Purple Mountain Observatory, Chinese Academy of Science, Nanjing 210008, China*

Received 29 October 2004; received in revised form 4 July 2005; accepted 16 July 2005

Abstract

The preliminary energy spectra of heavy nuclei C, O, Ne, Mg, Si, and Fe in the primary cosmic rays measured by the ATIC-2 experiment are presented and compared to previous data and to propagation models. Using previous data to extend the ATIC-2 results for all heavy nuclei to higher energy, the combined spectra can be best fit with diffusion model with weak reacceleration and scattering on random magnetic field with a Kolmogorov spectrum fluctuations becoming dominant at high energy.

Keywords: Cosmic rays; Heavy nuclei; Energy spectra; Propagation models

1. Introduction

ATIC (Advanced Thin Ionization Calorimeter) is a balloon borne experiment designed to measure cosmic ray composition for elements from hydrogen to iron and their energy spectra from 50 GeV to near 100 TeV. ATIC had two successful balloon flights in Antarctica: from 28 Dec 2000 to 13 Jan 2001 (test flight ATIC-1) and from 29 Dec 2002 to 18 Jan 2003 (science flight ATIC-2).

ATIC is comprised of a fully active bismuth germanate (BGO) calorimeter, a carbon target with embedded scintillator hodoscopes, and a silicon matrix that is used as a charge detector in the experiment (see Fig. 1). The detailed description of the ATIC spectrometer, and the method of calorimeter calibration may be found in Guzik et al. (2004). The description of the silicon matrix charge detector is given in Adams et al. (2001) and Zatsepin et al. (2004).

2. Charge resolution

In the experiment, the events selected are those in which a primary particle passes through the charge module, interacts in the carbon target, and generates an electron–hadron cascade in the calorimeter. An example of reconstruction of the trajectory and measurement of the charge are shown in Fig. 2. Upper left

* Corresponding author. Tel.: +7 095 939 3808.
E-mail address: panov@dec1.sinp.msu.ru (A.D. Panov).

0273-1177/$30 © 2005 COSPAR. Published by Elsevier Ltd. All rights reserved.
doi:10.1016/j.asr.2005.07.040

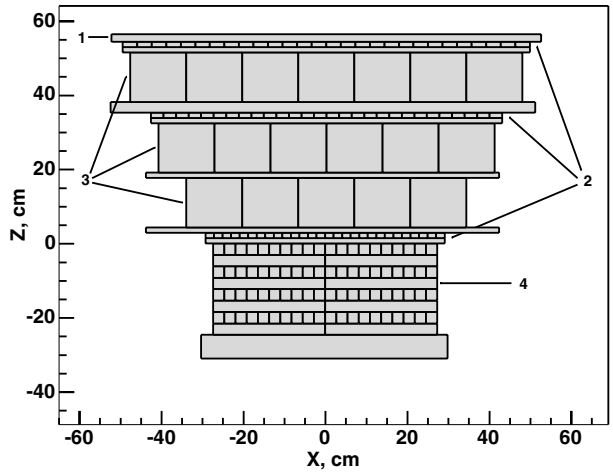

Fig. 1. Schematic view of the ATIC spectrometer: 1, silicon matrix; 2, scintillator hodoscopes; 3, carbon target; 4, BGO calorimeter.

graph in Fig. 2 represents the plane of the silicon charge detector. Rectangle on the silicon plane represents the error corridor for the reconstructed trajectory. Diamond denotes the primary particle that was found within the error corridor, triangle denotes the silicon pixel with the maximal energy deposit. The maximal silicon pixel and the pixel of primary particle is the same in Fig. 2. Lower left and upper right graphs in Fig. 2 are *XZ*- and *YZ*-projections of BGO calorimeter, respectively, with appropriate projections of the reconstructed trajectory. Sizes of little rectangles are proportional to the energy deposit in the appropriate BGO crystals. Since the BGO crystals in alternate layers are orthogonal (see Fig. 1), there are four X and four Y positions of the shower axis to be fit to determine the trajectory, which is then projected to the Si-matrix layer, as illustrated in Fig. 2. To fit the trajectory we used weighted least square method.

In the ATIC-2 exposure, the charge resolution was acceptable for all elements at all energies as illustrated in Fig. 3 for the region from B to Ni. The charge resolutions for some even heavy nuclei are presented in Table 1. Charge resolutions were calculated by approximation of charge peaks by gaussians (Fig. 4). We present here preliminary energy spectra for the heavy nuclei and compare the results to previous data and to models of cosmic ray propagation in the galaxy.

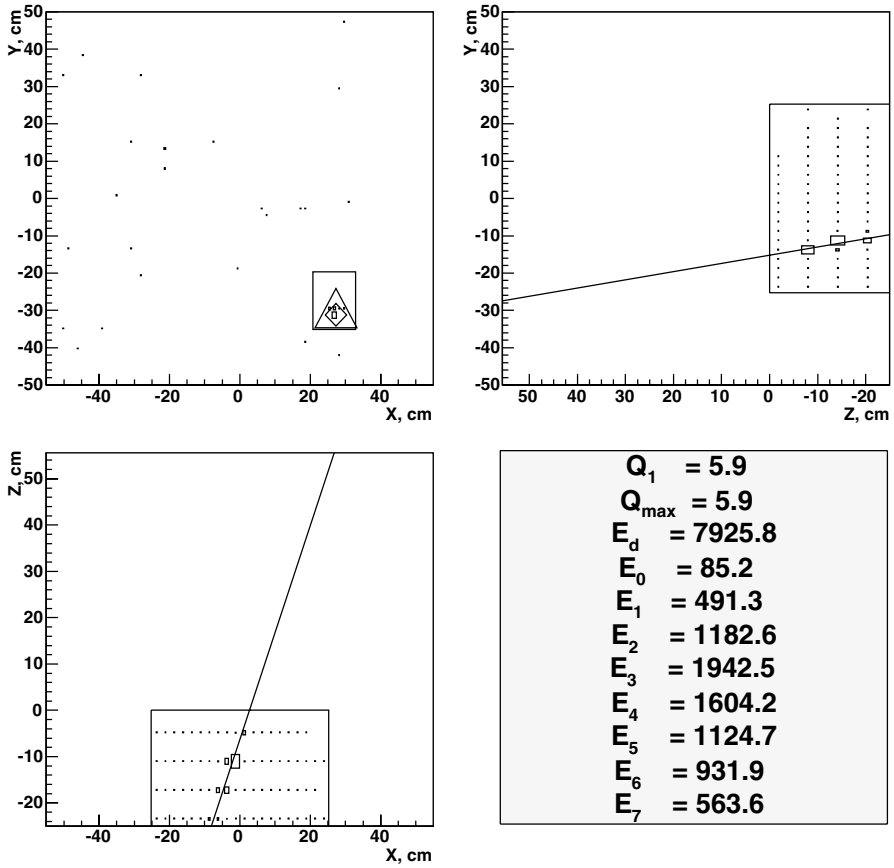

Fig. 2. An example of reconstruction of trajectory and measurement of particle charge. E_d, energy deposit in the calorimeter in GeV; Q_1, the charge of particle that was found within the error corridor of the trajectory; Q_{max}, the maximal charge in the whole silicon matrix (in this event Q_1 and Q_{max} are the same); E_0–E_7, energy deposits (in GeV) in the each of eight layers of the calorimeter.

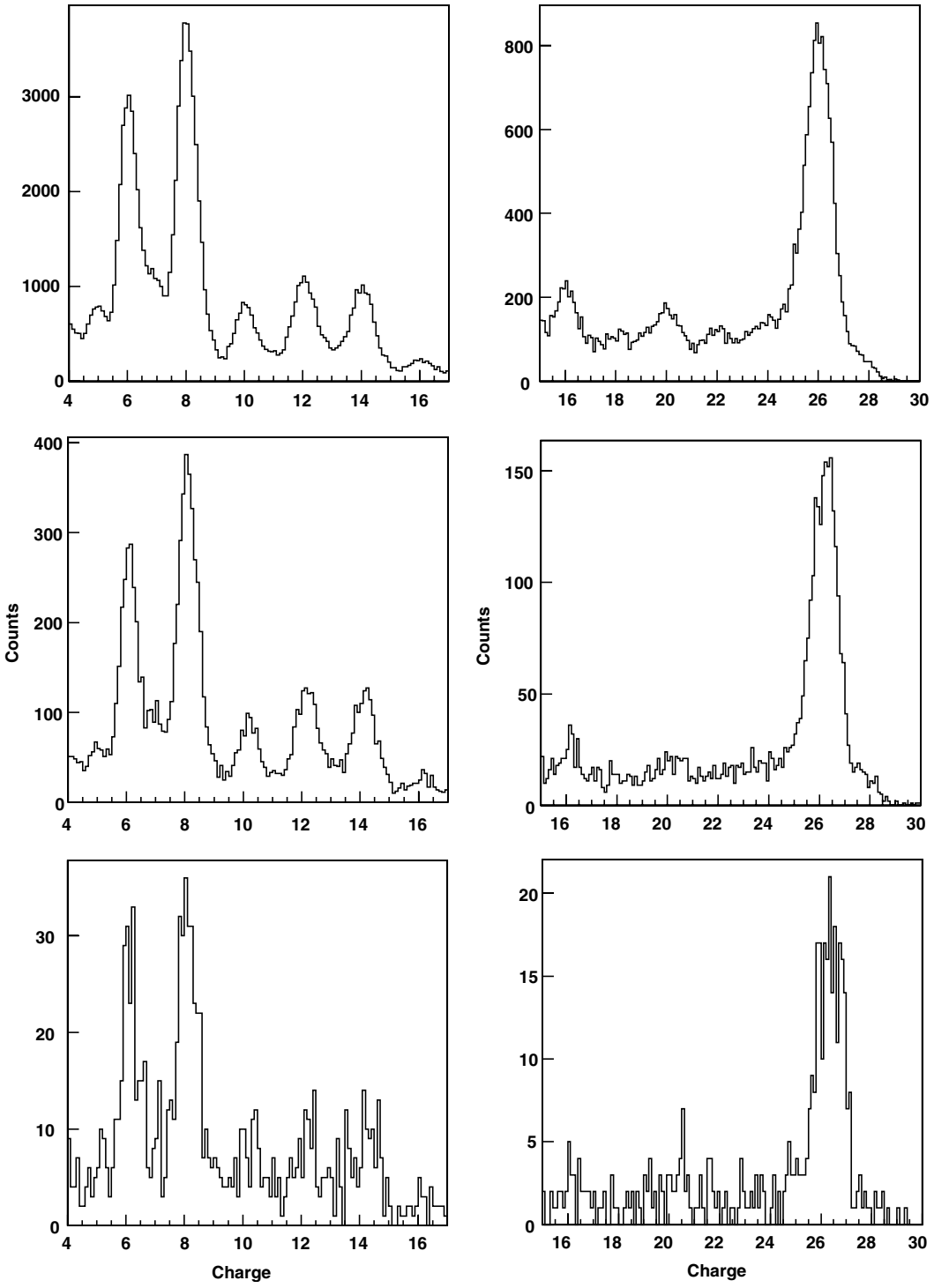

Fig. 3. Charge histograms for the heavy nuclei measured in ATIC-2 for different energy thresholds. First row is $E_d > 50$ GeV, second row is $E_d > 250$ GeV and third row is $E_d > 1000$ GeV.

3. Conversion to primary spectrum

The energy deposit E_d in the calorimeter in each reconstructed event is determined by summing the energy deposits in all BGO crystals. To convert a spectrum in E_d to spectrum in primary energy E, we adopt the approximation used in emulsion chamber calorimeter analysis (Burnett et al., 1986). A shift is used along the energy axis by k_s^{-1}, where

$$k_s = \int_0^1 k^{\gamma+1} \times f(k)\,dk \Big/ \int_0^1 k^{\gamma} \times f(k)\,dk.$$

Table 1
Charge resolutions for heavy nuclei at different energies

E_d (GeV)	C	O	Ne	Mg	Si
>50	0.29	0.29	0.31	0.34	0.35
>250	0.26	0.28	0.29	0.34	0.34
>1000	0.26	0.28	0.32	0.30	0.39

The represented values are the standard deviations of appropriate fitted gaussians in the units of proton charge.

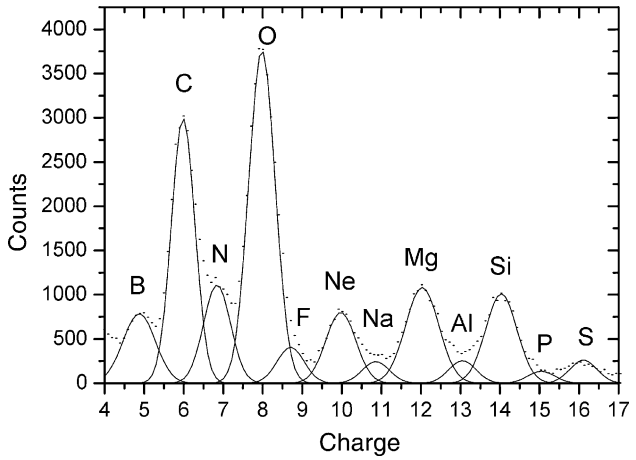

Fig. 4. Decomposition of the charge spectrum for $E_d > 50$ GeV by gaussians.

Here $f(k)$ is distribution of $k = E_d/E$ value at given E, and γ is the index of integral spectrum. The values of k_s were obtained using simulation of passing particles through ATIC with FLUKA code Fassó et al. (2001b), Fassó et al. (2001a) for different nuclei and for spectrum with $\gamma = 1.6$. The resulting k_s values are only weakly dependent on the choice of $\gamma = 1.6$. For a constant value of k_s, the spectral index is not altered between the E_d spectrum and E spectrum. Generally, k_s values depend on E due to leakage through the bottom and sides of the calorimeter. Our preliminary estimation shows that this dependence is weak, and leads to steepening of E_d spectrum by $\Delta\gamma = 0.04$. In the present paper, spectral shapes are presented without taking into account this correction factor, which needs to be refined. The fluxes were determined by the formula:

$$I = \frac{dN}{dE}/(S\Omega \times T \times \epsilon \times \eta \times W_{\text{eff}}),$$

where $S\Omega$ is geometry factor, T is exposure live time, ϵ is efficiency of event reconstructing algorithm, η is correction factor for attenuation in the residual atmosphere, and $W_{\text{eff}} = \int_0^1 k^\gamma f(k)\,dk/k_s^\gamma$. These values will be presented in more detail in a future paper.

It should be noted that this technique is only a first step toward accurate solution of the deconvolution problem to obtain energy spectra of primaries from the spectra of energy deposit. Therefore, the data of the present report should be considered as preliminary.

4. Results and discussion

The energy spectra (per nucleon) for abundant nuclei C, O, Ne, Mg, Si, Fe along with the data of HEAO-3-C2 experiment (Engelmann et al., 1990) and CRN experiment (Müller et al., 1991) are shown in Fig. 5. The agreement with the previous data is generally quite good.

To interpret the experimental spectra we use the Leaky Box approximation of the transport equation (Gaisser, 1990, pp. 119–122) to describe propagation of particles in the interstellar medium and transformation of primary spectra during propagation. The spectrum of a particle in this framework may be written as:

$$N_P(E) = \frac{Q_P(E)\tau_{\text{esc}}(R)}{1 + \lambda_{\text{esc}}(R)/\lambda_P}, \quad (1)$$

where $N_P(E)$ is the measured spectrum of particle P, $Q_P(E)$ is the spectrum at the source, R is the magnetic rigidity of the particle, $\lambda_{\text{esc}}(R)$ is the mean amount of matter traversed by a particle without nuclear fragmentation process, λ_P is the fragmentation length, and $\tau_{\text{esc}} = \lambda_{\text{esc}}/(v\rho)$. In the last formula v is the velocity of the particle and ρ is density of the interstellar medium.

In the HEAO3-C2 experiment (Engelmann et al., 1990) it was shown that the experimental data for energies below 35 GeV/n can be described by the Leaky Box model with a source spectrum in the shape of a power law in momentum with a spectral index 2.23, and B/C ratio data of HEAO produces the following dependency $\lambda_{\text{esc}}(R)$ (Engelmann et al., 1990):

$$\begin{cases} \lambda_{\text{esc}} = 34.1\beta R^{-0.6}\ \text{g cm}^{-2}, & R > 4.4\ \text{GV} \\ \lambda_{\text{esc}} = 14.0\beta, & R < 4.4\ \text{GV}. \end{cases} \quad (2)$$

The predictions of the model Eqs. (1) and (2) are shown as dashed lines compared to the data in Fig. 5. The agreement is acceptable, but the dashed curves appear to underestimate the ATIC-2 data, particularly C and O at the highest energies.

The Leaky Box is a popular empirical model which stands out because of its simplicity. In the application to the case of stable energetic nuclei, the Leaky Box equations can be derived as an approximation to the equations obtained in the flat-halo diffusion model without reacceleration. The energy dependence of the escape length is determined then by the energy dependence of cosmic ray diffusion coefficient D: $\lambda_{\text{esc}} \propto v/D$.

The power law form of λ_{esc} Eq. (2) implies a very short escape length at high energies and this would imply a larger anisotropy than has been observed (Erlykin et al., 1998). However, in the paper (Osborne and Ptuskin, 1988), it was shown that the form of Eq. (1)

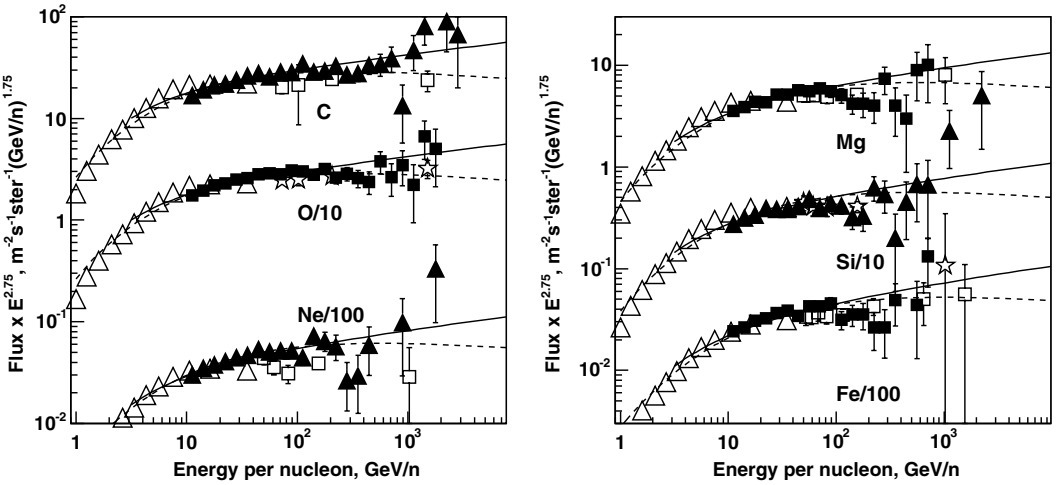

Fig. 5. Energy spectra (per nucleon) for even abundant nuclei. Open triangles, the data of HEAO-3-C2 (Engelmann et al., 1990); open squares and open stars, the data of CRN (Müller et al., 1991); filled marks, data of ATIC-2. The curves show results of propagation calculations as discussed in the text.

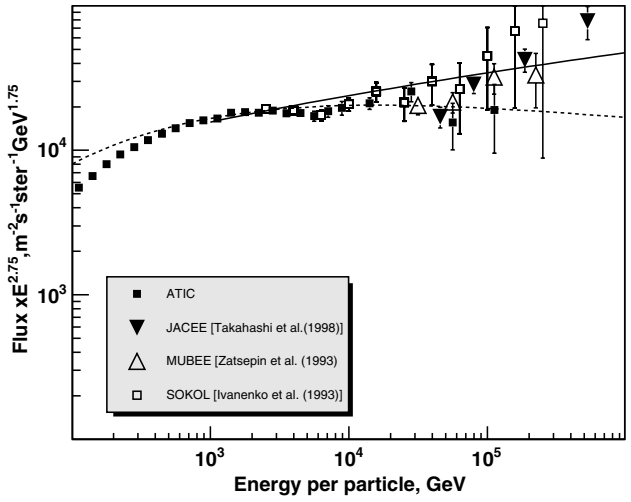

Fig. 6. Energy spectra (per particle) for all nuclei heavier than Boron. The curves show propagation model calculations as described in the text.

is also correct for a diffusion model with weak reacceleration during propagation due to cyclotron resonance scattering of the particles, if λ_{esc} is replaced with effective thickness x_{eff}. According to Osborne and Ptuskin (1988):

$$x_{\mathrm{eff}}(R) = 4.2 \times (R/R_0)^{-1/3} \times (1 + (R/R_0)^{-2/3}) \ \mathrm{g/cm^2} \quad (3)$$

where $R_0 = 5.5$ GV. This equation corresponds to the scattering on random magnetic field with a Kolmogorov spectrum at high energies (Ptuskin, 2001). In such a form the expected anisotropy at high energies does not contradict the experimental data. The prediction of the model Eqs. (1) and (3) for the spectrum at the source $Q_P(E) \propto E^{-2.3}$ is shown in Fig. 5 by solid line. This improves the fit to the individual element spectra at highest energies but the statistics are not sufficient to make definite conclusions.

To improve the statistics at the highest energy, Fig. 6 shows a plot of all nuclei heavier than Boron, as a function of energy per particle. The ATIC-2 results are compared to the data from JACEE (Takahashi et al., 1998), MUBEE (Zatsepin et al., 1993), and SOKOL (Ivanenko et al., 1993). The ATIC-2 results are in good agreement with the SOKOL results below 30 TeV. In the energy range higher than 30 TeV the statistics of the ATIC data are too poor to make choice between the simple Leaky Box model and the model Eqs. (1) and (3). However, it is visible that simple Leaky Box model with power law for λ_{esc} as in Eqs. (1) and (2) falls below other experimental data at the highest energies. All the variety of the experimental data definitely points out to better agreement with the model Eqs. (1) and (3).

5. Conclusions

The ATIC-2 results on the spectra of heavy nuclei are in agreement with previous data from HEAO, CRN, and Sokol. The results can be explained with the leaky box model but the diffusion model with weak reacceleration produces better fit to the experimental data. The ATIC results are still preliminary and further analysis is underway.

Acknowledgements

The work was supported by Russian Foundation for Basic Research Grant Nos. 99-02-16246 and 02-02-16545 in Russia, NASA Grant Nos. NAG5-5064,

NAG5-5306, NAG5-5155, NAG5-5308 and the NASA SR&T program in the USA, and the Chinese Academy of Sciences and the Max-Planck Institute.

References

Adams, J.H., Bashindzhagyan, G.L., Zatsepin, V.I., Merkin, M.M., Panasyuk, M.I., Samsonov, G.A., Sokol'skya, N.V., Khein, L.A. The silicon matrix as a charge detector for the ATIC experiment. Instrum. Exp. Tech. 44 (4), 455–461, 2001.

Burnett, T.H., Dake, S., Fuki, M., et al., JACEE Collaboration. Jacee emulsion chambers for studying the energy spectra of high energy cosmic ray protons and helium. Nucl. Instr. Meth. A 251, 583–595, 1986.

Engelmann, J.J., Ferrando, P., Soutoul, A., et al., HEAO Collaboration. Charge composition and energy spectra of cosmic-ray nuclei for elements from Be to Ni. results from HEAO-3-C2. Astron. Astrophys. 233, 96–111, 1990.

Erlykin, A.D., Lipsky, M., Wolfendale, A.W. Hight energy cosmic ray spectroscopy. IV. The evidence from direct observation at lower energies and directional anisotropies. Astropart. Phys. 8, 283–292, 1998.

Fassó, A., Ferrari, A., Ranft, J., Sala, P.R. FLUKA: Status and prospective for hadronic applications, in: Kling, A., Barao, F., Nakagawa, M., Tavora, L., Vaz, P. (Eds.), Proceedings of the MonteCarlo 2000 Conference, Lisbon, October 23–26, 2000. Springer-Verlag, Berlin, pp. 955–960, 2001a.

Fassó, A., Ferrari, A., Sala, P.R. Electron–photon transport in FLUKA: status, in: Kling, A., Barao, F., Nakagawa, M., Tavora, L., Vaz, P. (Eds.), Proceedings of the MonteCarlo 2000 Conference, Lisbon, October 23–26, 2000. Springer-Verlag, Berlin, pp. 159–164, 2001b.

Gaisser, T.K. Cosmic Rays and Particle Physics. Cambridge University Press, New Yourk, Port Chester, Melbourn, Sydney, 1990.

Guzik, T.G., Adams, J.H., Ahn, H.S., et al., ATIC Collaboration. The ATIC long duration balloon project. Adv. Space Res. 33 (10), 1763–1770, 2004.

Ivanenko, I.P., Shestoperov, V.Y., Chikova, L.O., et al. Energy spectra of cosmic rays above 2 TeV as measured by the "Sokol" apparatus, in: Proceedings of the 23rd International Cosmic Ray Conference, vol. 2, Calgary, pp. 17–20, 1993.

Müller, D., Swordy, S.P., Meyer, P., L'Heureux, J., Grunsfeld, J.M. Energy spectra and composition of primary cosmic rays. Astrophys. J. 374, 356–365, 1991.

Osborne, J.L., Ptuskin, V.S. Cosmic-ray reacceleration in the interstellar medium. Sov. Astron. Lett. 14 (2), 132–134, 1988.

Ptuskin, V.S. Cosmic ray origin: general overview, in: Shapiro, M.M. (Ed.), Astrophysical sources of High Energy Particles and Radiation. Kluwer Academic Publishers, Netherlands, pp. 251–262, 2001.

Takahashi, Y. et al., JACEE Collaboration. Elemental abundance of high energy cosmic rays. Nucl. Phys. B (Proc. Suppl.) 60B, 83–92, 1998.

Zatsepin, V.I., Adams, J.H., Ahn, H.S., et al., ATIC Collaboration. The silicon matrix as a charge detector in the ATIC experiment. Nucl. Instr. Meth. A 524, 195–207, 2004.

Zatsepin, V.I., Zamchalova, E.A., Varkovitskaya, A.Y., Sokolskaya, N.V., Sazhina, G.P., Lazareva, T.V. Energy spectra of primary protons and other nuclei in energy region 10–100 TeV/nucleus, in: Proceedings of the 23rd ICRC, vol. 2, pp. 13–16, 1993.